Springer

Dear Author,

Here are the proofs of your article.

- You can submit your corrections **online**, via **e-mail** or by **fax**.
- For **online** submission please insert your corrections in the online correction form. Always indicate the line number to which the correction refers.
- You can also insert your corrections in the proof PDF and **email** the annotated PDF.
- For fax submission, please ensure that your corrections are clearly legible. Use a fine black pen and write the correction in the margin, not too close to the edge of the page.
- Remember to note the **journal title**, **article number**, and **your name** when sending your response via e-mail or fax.
- **Check** the metadata sheet to make sure that the header information, especially author names and the corresponding affiliations are correctly shown.
- **Check** the questions that may have arisen during copy editing and insert your answers/ corrections.
- **Check** that the text is complete and that all figures, tables and their legends are included. Also check the accuracy of special characters, equations, and electronic supplementary material if applicable. If necessary refer to the *Edited manuscript*.
- The publication of inaccurate data such as dosages and units can have serious consequences. Please take particular care that all such details are correct.
- Please **do not** make changes that involve only matters of style. We have generally introduced forms that follow the journal's style.
  Substantial changes in content, e.g., new results, corrected values, title and authorship are not allowed without the approval of the responsible editor. In such a case, please contact the Editorial Office and return his/her consent together with the proof.
- If we do not receive your corrections **within 48 hours**, we will send you a reminder.
- Your article will be published **Online First** approximately one week after receipt of your corrected proofs. This is the **official first publication** citable with the DOI. **Further changes are, therefore, not possible.**
- The **printed version** will follow in a forthcoming issue.

Please note

After online publication, subscribers (personal/institutional) to this journal will have access to the complete article via the DOI using the URL: http://dx.doi.org/[DOI].
If you would like to know when your article has been published online, take advantage of our free alert service. For registration and further information go to: http://www.link.springer.com.

Due to the electronic nature of the procedure, the manuscript and the original figures will only be returned to you on special request. When you return your corrections, please inform us if you would like to have these documents returned.

Metadata of the article that will be visualized in OnlineFirst

ArticleTitle	Influence of an Arterial Stenosis on the Hemodynamics Within an Arteriovenous Fistula (AVF): Comparison Before and After Balloon-Angioplasty	
Article Sub-Title		
Article CopyRight	Biomedical Engineering Society (This will be the copyright line in the final PDF)	
Journal Name	Cardiovascular Engineering and Technology	
Corresponding Author	Family Name	**Salsac**
	Particle	
	Given Name	**Anne-Virginie**
	Suffix	
	Division	Biomechanics and Bioengineering Laboratory (UMR CNRS 7338)
	Organization	Université de Technologie de Compiègne
	Address	CS 60319, Compiègne Cedex, 60203, France
	Email	a.salsac@utc.fr
Author	Family Name	**Decorato**
	Particle	
	Given Name	**Iolanda**
	Suffix	
	Division	Biomechanics and Bioengineering Laboratory (UMR CNRS 7338)
	Organization	Université de Technologie de Compiègne
	Address	CS 60319, Compiègne Cedex, 60203, France
	Email	
Author	Family Name	**Legallais**
	Particle	
	Given Name	**Cecile**
	Suffix	
	Division	Biomechanics and Bioengineering Laboratory (UMR CNRS 7338)
	Organization	Université de Technologie de Compiègne
	Address	CS 60319, Compiègne Cedex, 60203, France
	Email	
Author	Family Name	**Alimohammadi**
	Particle	
	Given Name	**Mona**
	Suffix	
	Division	Mechanical Engineering Dept
	Organization	University College London
	Address	Torrington Place, London, WC1E 7JE, UK
	Email	
Author	Family Name	**Diaz-Zuccarini**
	Particle	
	Given Name	**Vanessa**
	Suffix	

	Division	Mechanical Engineering Dept
	Organization	University College London
	Address	Torrington Place, London, WC1E 7JE, UK
	Email	
Author	Family Name	**Kharboutly**
	Particle	
	Given Name	**Zaher**
	Suffix	
	Division	Biomechanics and Bioengineering Laboratory (UMR CNRS 7338)
	Organization	Université de Technologie de Compiègne
	Address	CS 60319, Compiègne Cedex, 60203, France
	Email	

Schedule	Received	9 January 2013
	Revised	
	Accepted	5 May 2014

Abstract	The study focuses on arterial stenoses in arteriovenous fistulae (AVF), the occurrence of which was long underestimated. The objective is to investigate their influence on the hemodynamic conditions within the AVF. A numerical simulation of the blood flow is conducted within a patient-specific arteriovenous fistula that presents an 60% stenosis on the inflow artery. In order to find the vessel shape without stenosis and compare the flow conditions with and without stenosis, the endovascular treatment of balloon-angioplasty is simulated by modeling the vessel deformation during balloon inflation implicitly.Clinically, balloon-angioplasty is considered successful if the post-treatment residual degree of stenosis is below 30%. Different balloon inflation pressures have been imposed numerically to obtain residual degrees of stenosis between 30 and 0%. The comparison of the computational fluid dynamic simulations carried out in the patient-specific native geometry and in the treated ones shows that the arterial stenosis has little impact on the blood flow distribution. The venous flow rate remains unchanged as long as thrombosis does not occur: the nominal flow rate needed for hemodialysis is maintained, which is not the case for a venous stenosis. An arterial stenosis, however, causes an increase in the pressure difference across the stenosed region. A residual degree of stenosis below 20% is needed to guarantee a pressure difference lower than 5 mmHg, which is considered to be the threshold stenosis pressure difference.

Keywords (separated by '-')	Arteriovenous fistula - Stenosis - Balloon-angioplasty - Hemodynamics - Stenosis pressure drop
Footnote Information	Associate Editor Ajit P. Yoganathan oversaw the review of this article. MeDDiCA ITN (Marie Curie Actions, grant agreement PITN-GA-2009-238113).

Cardiovascular Engineering and Technology (© 2014)
DOI: 10.1007/s13239-014-0185-7

Influence of an Arterial Stenosis on the Hemodynamics Within an Arteriovenous Fistula (AVF): Comparison Before and After Balloon-Angioplasty

IOLANDA DECORATO,[1] ANNE-VIRGINIE SALSAC,[1] CECILE LEGALLAIS,[1] MONA ALIMOHAMMADI,[2] VANESSA DIAZ-ZUCCARINI,[2] and ZAHER KHARBOUTLY[1]

[1]Biomechanics and Bioengineering Laboratory (UMR CNRS 7338), Université de Technologie de Compiègne, CS 60319, 60203 Compiègne Cedex, France; and [2]Mechanical Engineering Dept, University College London, Torrington Place, London WC1E 7JE, UK

(Received 9 January 2013; accepted 5 May 2014)

Associate Editor Ajit P. Yoganathan oversaw the review of this article.

Abstract—The study focuses on arterial stenoses in arteriovenous fistulae (AVF), the occurrence of which was long underestimated. The objective is to investigate their influence on the hemodynamic conditions within the AVF. A numerical simulation of the blood flow is conducted within a patient-specific arteriovenous fistula that presents an 60% stenosis on the inflow artery. In order to find the vessel shape without stenosis and compare the flow conditions with and without stenosis, the endovascular treatment of balloon-angioplasty is simulated by modeling the vessel deformation during balloon inflation implicitly.Clinically, balloon-angioplasty is considered successful if the post-treatment residual degree of stenosis is below 30%. Different balloon inflation pressures have been imposed numerically to obtain residual degrees of stenosis between 30 and 0%. The comparison of the computational fluid dynamic simulations carried out in the patient-specific native geometry and in the treated ones shows that the arterial stenosis has little impact on the blood flow distribution. The venous flow rate remains unchanged as long as thrombosis does not occur: the nominal flow rate needed for hemodialysis is maintained, which is not the case for a venous stenosis. An arterial stenosis, however, causes an increase in the pressure difference across the stenosed region. A residual degree of stenosis below 20% is needed to guarantee a pressure difference lower than 5 mmHg, which is considered to be the threshold stenosis pressure difference.

Keywords—Arteriovenous fistula, Stenosis, Balloon-angioplasty, Hemodynamics, Stenosis pressure drop.

Address correspondence to Anne-Virginie Salsac, Biomechanics and Bioengineering Laboratory (UMR CNRS 7338), Université de Technologie de Compiègne, CS 60319, 60203 Compiègne Cedex, France. Electronic mails: a.salsac@utc.fr and anne-virginie.salsac@utc.fr

MeDDiCA ITN (Marie Curie Actions, grant agreement PITN-GA-2009-238113).

INTRODUCTION

An arteriovenous fistula (AVF) is a permanent vascular access created surgically in patients with end-stage renal disease waiting for kidney transplantation.[22] It enables circulating blood extra-corporeally to a filtering machine during the sessions of hemodialysis: blood is cleaned from metabolic waste products and excess of water.[19] The most common approach used to create the arteriovenous fistula is to suture a vein onto an artery in the forearm or in the arm. Autologous fistulas have a 3- to 6-month maturation, during which the vein dilates and the wall collagen content increases.[8,10] Over maturation, the venous flow rate increases by a factor 20–50 and reaches a value larger than 500 mL/min, which is required for hemodialysis.[22,40] The fistula acts as a short-cut between the high pressure arterial vasculature and the low pressure venous tree causing a significant change of the hemodynamic conditions.

The issue is that more than half the AVF fail within 2 years.[4] Loss of patency of the vascular access can result in underdialysis, leading to increased morbidity and mortality. For many years venous stenoses (also called outflow stenosis) were considered to be the main complication affecting arteriovenous fistulas.[7,23] They typically form in the draining vein near the vein-to-artery junction (called the anastomosis) or in the central veins located downstream of the anastomosis.[28,37] Coentrao and Turmel-Rodrigues pointed out that venous stenoses are so common that many clinicians do not diagnose their presence.[7] They directly compromise the hemodialysis treatment, because they

reduce the venous blood flow or even block it when they cause thrombosis.[14]

For a long time, the occurrence of arterial inflow stenoses was considered a rare complication in hemodialysis fistula.[36] Recent studies have, however, provided a very different picture of the reality. Arterial stenoses have been shown to occur in 40% of patients when the AVF is created in the forearm.[2,11] The occurrence rate is lower when the AVF is in the upper arm (presumably around 0–4%). Relatively little is known about arterial stenoses. Indeed they remain often undiagnosed because they hardly affect the parameters monitored during hemodialysis, unless they are close to the anastomosis.[31,34] They could easily be detected by ultrasound scans or angiography, but neither are part of the routine exam conducted on hemodialyzed patients.

If detected, correction of the arterial stenosis needs to be considered before thrombosis and vascular access loss. The indications for treatment are so far the same as for venous stenoses: a lumen narrowing greater than 50% or a pressure drop higher than 5 mmHg.[2,14] The lumen criterion is thought to be universally valid[14] but less can be said on the critical pressure drop across an arterial stenosis. The stenosis can be treated either surgically or endovascularly, the former being more invasive and usually performed when the vascular anatomy is likely to affect the success rate of the endovascular procedure.[37] Balloon-angioplasty is the endovascular treatment of choice: it consists in inflating a balloon to restore the stenosed vessel patency. After treatment, the diameter at the stenosis throat is rarely restored to its physiological value, and a residual stenosis remains. Treatment is considered successful when the degree of residual stenosis is below 30%.[3,6,14,37]

The objective of the study is to provide a better understanding of the consequences of an arterial stenosis. We aim at investigating its influence on the hemodynamic conditions in a patient-specific AVF: the blood flow conditions are hence compared with and without the lesion. The approach used is based on computational fluid-dynamic (CFD) simulations, which have been reported to be effective in the evaluation of the AVF hemodynamics.[12,21,27] Previous studies have, however, not yet investigated the consequences of a stenosis in a fistula. Numerical simulations present the advantage of providing quantitative information on flow parameters such as the wall shear stress and stenosis pressure difference that cannot be measured *in vivo*. Such information can be useful to set the guidelines for the treatment of arterial stenoses in AVF, which so far do not exist. The treatment of balloon-angioplasty is simulated numerically to get the post-treatment vascular geometry in the case of degrees of residual stenosis ranging from 30 to 0%. A technique is proposed to set patient-specific boundary conditions from the only clinical data that can be measured *in vivo* on the patients, i.e., the flow rates.

The manuscript is structured as follows. The techniques used to generate the patient-specific vessel geometry, simulate balloon-angioplasty and conduct computational fluid dynamic studies are detailed in §2, along with the validation of the numerical simulations. In §3, we compare the geometries and flow conditions before and after balloon-angioplasty. The evolution of the hemodynamic flow parameters is studied as a function of the degree of post-treatment residual stenosis. We conclude with a discussion on the possible clinical implications of the study.

METHODS

Patient-Specific Geometry

The investigated vasculature consisted of a mature side-to-end radio-cephalic AVF created in a patient with end-stage renal failure. The vascular lumen was segmented and reconstructed from medical images. The images were obtained by computed tomography (CT) scan angiography on a patient that was at rest in supine position at the Polyclinique St Côme (Compiègne, France). In order to visualize blood in the artery and in the vein during the same acquisition, a contrast bolus was injected in the patient opposite arm. The amount of contrast agent was dosed to optimize the image contrast and resolution in both vessels. The best volume reconstruction was obtained by applying a combination of intensity and gradient forces and a smoothness constraint based on the curvature of the surface.[21] The reconstructed vascular geometry is shown in Fig. 1: it presents an 60% stenosis on the arterial side. Throughout the manuscript, the subscript *a* refers to the arterial part of the AVF, the subscript *v* to the vein, the superscript *i* to the inlet of the vessel and the superscript *o* to the outlet.

Numerical Method to Simulate Balloon-Angioplasty

Numerical Procedure

The treatment by balloon-angioplasty was simulated numerically using ANSYS-Structural (ANSYS, Inc.). Our objective was not to study the transient balloon deformation, but to obtain the equilibrium configuration of the stenosed wall. We hence used an implicit formulation of the solid problem, which is one of the original aspects of the study. A balloon was positioned across the stenosis; it was inflated (and deflated) by imposing an internal pressure in an

Journal : CVET MS Code : 13239 PIPS No. : 185 ☐ TYPESET ☑ DISK ☐ LE ☑ CP Dispatch : 8-5-2014 Pages : 11

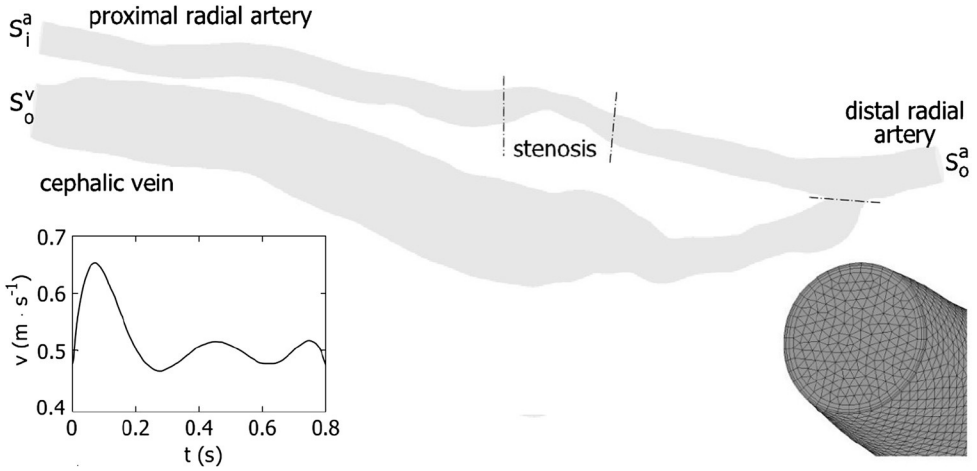

FIGURE 1. Geometry of the patient-specific arteriovenous fistula. The surface S_a^i is the arterial inlet section, S_a^o the arterial outlet section and S_v^o the venous outlet section. The dotted lines indicate the separation between the stenosed and non-stenosed regions of the artery and the separation between the artery and vein. The insert on the left shows the velocity waveform v_a^i set at the arterial inlet (S_a^i); it was been measured on the patient by echo-Doppler. The insert on the right is a magnification of the mesh at the distal arterial outlet (S_a^o).

implicit structural simulation. The simulation was conducted with the Lagrangian multiplier-based mixed deformation-pressure numerical scheme (u-P formulation). Neither translation nor rotation was allowed at the extremities of the balloon and vessel walls. The convergence criteria on force, momentum, displacement and rotation were set to be 10^{-4}. In all the simulations (solid and fluid), the reference pressure was the atmospheric pressure, which was set to zero to obtain gauge pressure results. No wrinkle was observed on the balloon, since the inner balloon pressure also remained higher than the outer pressure.

Modeling of the Angioplasty Balloon

The balloon was modeled as a cylinder with linear elastic mechanical properties. It was created as a separate body using ANSYS FE-Modeler (ANSYS, Inc.) It was meshed with a monolayer of discrete-Kirchhoff theory-based, four-node linear-triangular shell finite elements and positioned across the stenosis as shown in Fig. 2a. The balloon Young modulus was set at 9×10^8 Pa.[16] A Poisson coefficient of 0.3 was imposed to guarantee numerical convergence.

Modeling of the Arterial Vessel

For the simulation of balloon-angioplasty, only the portion around the stenosed artery was modeled. The simulated zone had a total length of 4.2 cm and was centered onto the stenosis. No direct measurement of wall thickness were possible *in vivo*. Measurements in arteries of similar caliber found the thickness to be about 1/10th of the arterial diameter.[18] The thickness of the non-stenosed artery was therefore set to be 0.6 mm. In the stenosed part, an average thickness value equal to 0.8 mm was imposed. The vascular wall was meshed with a monolayer of discrete-Kirchhoff theory-based, four-node linear-triangular shell finite elements. Prior to meshing, the AVF wall was sub-divided in order to impose different mechanical properties to the healthy artery and to the stenosed arterial portion (Fig. 1).

The non-stenosed parts of the artery were assumed to be incompressible and to follow the 3rd-order Yeoh model.[39] The associated strain energy function ψ was

$$\psi = C_{10}(I_1 - 3) + C_{20}(I_1 - 3)^2 + C_{30}(I_1 - 3)^3 \quad (1)$$

with I_1 the deviatoric first principal strain invariant. The material constants were found by best-fitting experimental data obtained on healthy arteries[29]: $C_{10} = 0.763 \times 10^5$ Pa, $C_{20} = 3.697 \times 10^5$ Pa, $C_{30} = 5.301 \times 10^5$ Pa (coefficient of determination $R^2 = 0.985$).

The stenosed part of the artery was modeled with the Maxwell model, which is a viscoplastic model composed of an elastic spring in series with a viscous dashpot. The law parameters were chosen following two criteria. We imposed that the stenosed and non-stenosed parts of the artery had the same stiffness at small deformation in order to ensure mechanical continuity at the interface between them. At large deformations the parameter values were set in order to fit the data of Maher *et al.*[24]

Description of the Various Stages of the Simulation

At each instant of time, the structural simulation consisted in finding the mechanical equilibrium between the deformable artery and the elastic balloon

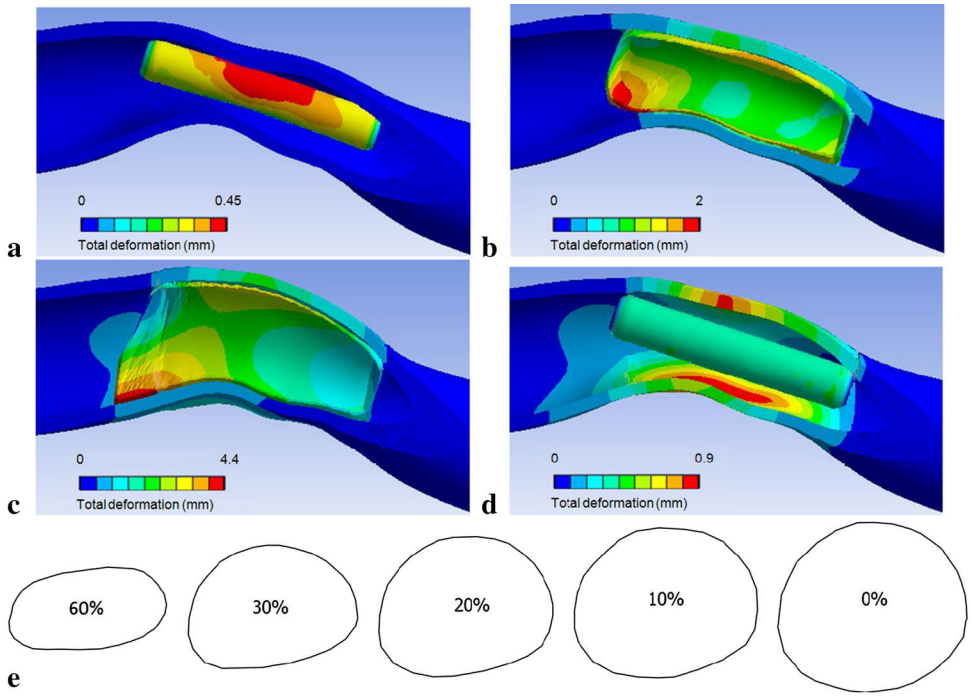

FIGURE 2. Snapshots of the evolution of the artery shape during the numerical simulation of balloon-angioplasty. (a) Initial configuration. (b) Configuration when the balloon comes into contact with the artery. (c) Configuration at maximum balloon internal pressure. (d) Vessel final shape when the balloon is completely deflated. (e) Vessel cross-sections at the throat of the stenosis for the patient-specific (60%-stenosis) and treated geometries (30, 20, 10, 0% residual stenosis).

implicitly. The vessel residual stresses were neglected due to a lack of existing data: to estimate them, the unloaded vessel geometry would have needed to be determined, since the artery was under pressure and already stretched when the imaging data were obtained *in vivo*. But such a process was not feasible in the case of a stenosed vessel, as no information was known on the actual wall thickness and properties in the stenosed region. It is likely that assuming zero residual stress mainly affects the balloon inflation pressures needed to reach the targeted degree of residual stenosis. But one can hypothesize that it will have a negligible effect on the actual vessel shape that is obtained.

At the beginning of the simulation the balloon was not in contact with the artery (Fig. 2a). The balloon was inflated by an increasing linear ramp in pressure. Figure 2b shows when contact occurred between the balloon and arterial wall. The contact problem was solved using the augmented-Lagrange method; it was supposed to be frictionless.[15] The balloon was further inflated until the maximum pressure was reached (Fig. 2c). It was then deflated following a decreasing linear pressure ramp, leaving the vessel wall in its post-treatment configuration (Fig. 2d). Different values of the balloon pressure were imposed (6, 5.6, 5.1, 4.7 bar). They respectively led to a degree of residual stenosis equal to 0, 10, 20 and 30% after angioplasty (Fig. 2e).

Numerical Method to Simulate the Hemodynamics Inside the AVF

Numerical Procedure

ANSYS-CFX (ANSYS, Inc.) was used to solve the continuity and momentum equations in their conservative convection-diffusion form.[1] The equations were solved implicitly with the Rhie-Chow interpolation method.[30] We used the high-resolution, second-order backward Euler scheme implemented in the ANSYS-CFX fluid solver (ANSYS, Inc.). It is an implicit time-stepping scheme recommended for non-turbulent flow simulations.[1] The system of algebraic equations was solved iteratively using a time-step Δt equal to 5 ms. At each time step, the residual was calculated and reported as a measure of the overall conservation of the flow properties. The maximum residual allowed was 10^{-4}. Convergence was verified in less than 10 sub-iterations at the first time step and in less than five iterations at all the following time steps.

Modeling of Blood in the Lumen

The patient-specific lumen was meshed starting from the triangulation of the lateral face of the reconstructed AVF lumen (right insert in Fig. 1). The mesh was made of an hybrid grid created in ANSYS T-Grid. First the boundary layer was meshed with seven

Journal : CVET MS Code : 13239 PIPS No. : 185 ☐ TYPESET ☑ DISK ☐ LE ☑ CP Dispatch : 8-5-2014 Pages : 11

layers of prismatic elements of decreasing thickness along the radius. The core was then meshed with tetrahedrons. Both cell element types were linear.

Blood was assumed to be an isotropic homogeneous non-Newtonian fluid. Modeling blood with a non-Newtonian model is justified by the low shear rate conditions that prevail inside the cephalic vein: the wall shear stresses in this region would have otherwise been overestimated by a Newtonian model. The blood apparent viscosity μ was assumed to follow the Casson model:

$$\sqrt{\mu} = \sqrt{\frac{\tau_0}{\dot{\gamma}}} + \sqrt{\kappa}. \quad (2)$$

where τ_0 represents the yield stress, $\dot{\gamma}$ the shear rate and κ the consistency. Blood density was set at 1050 kg m^{-3}. The model parameters were chosen according to experimental data obtained at low shear rates: $\tau_0 = 4 \times 10^{-3}$ Pa, $\kappa = 3.2 \times 10^{-3}$ Pa s.[25]

Boundary Conditions

A time-dependent velocity v_a^i was set at the arterial inlet S_a^i: it was measured by echo-Doppler in the proximal radial artery of the patient on the day of the CT-scan (Fig. 1). The measurements corresponded to a systolic Reynolds number of 1230, a time-averaged Reynolds number of 1020 (time-averaged inlet flow rate $\overline{Q}_a^i = 1.1$ L min^{-1}) and a Womersley number of 4. The inlet velocity was imposed as a flat velocity profile.

At each of the two outlets S_a^o and S_v^o, a Windkessel model was imposed, which consists in imposing a pressure-flow relationship as boundary condition.[38] The Windkessel model is based on the hypothesis that the blood flow is a function of the compliance and resistance of the network. If one models the vessel compliance as a capacitor and the hydraulic resistance as an electrical resistance, one can generate a zero-dimensional model of the flow in the network through a simple electrical analog circuit.

The behavior of the downstream vasculature was presently modeled with a capacitor C in parallel with a resistance R. The relationship between the blood flow rate Q and the pressure P was then given by

$$\frac{\partial P}{\partial t} = \frac{Q - \frac{P}{R}}{C}. \quad (3)$$

The equation was discretized using a first-order scheme.

The method set by Molino *et al.*[26] to estimate the parameters R and C, requires knowing

- the pulse pressure, defined as the difference between the systolic pressure P_s and the diastolic pressure P_d at the considered outlet;
- the time-averaged pressure $\overline{P}$ at the flow outlet;
- the time-averaged blood flow rate $\overline{Q}$ at the same flow outlet.

The time-averaged flow rate was known from the *in vivo* measurements by echo-Doppler, but neither the pulse pressure nor the time-averaged pressure were allowed to be measured on the patient, as pressure measurements are invasive and are not part of the patient regular follow-up. The only solution to estimate the pulse pressure and pressure drop along the AVF was to use simulation. A flow simulation was run imposing the measured flow rate at the inlet, the measured flow split between the arterial and venous outlets and constant outlet pressures at sections S_a^o and S_v^o. It provided a pulse pressure $P_s - P_d = 12$ mmHg.

To get the time-averaged pressures at the flow outlets, $\overline{P}_a^o$ and $\overline{P}_v^o$, from the calculated value of the pressure drop along the AVF, we searched the literature for the value of the mean pressure in the proximal radial artery in AVF patients: functional fistulas have an inlet mean pressure, which can vary between 50 and 100 mmHg,[5] depending on the patient general health conditions. To cover the whole possible range, different values of time-averaged inlet pressure $\overline{P}_a^i$ were chosen. Table 1 provides the R and C values that were calculated at the arterial and venous outlets for each value of $\overline{P}_a^i$ using the Molino *et al.* method.[26]

The same R and C values were used for all the simulations, both before and after the treatment by angioplasty. The post-angioplasty simulations therefore model the situation shortly after treatment, before the occurrence of any physiological adaptation in the distal circulation.

Initial Conditions

The velocity field was initialized with the solution of the steady-state simulation. In this simulation the fluid properties were identical to the ones described above. As boundary conditions, we imposed the time-averaged values of the inlet velocity at S_a^i and the time-averaged values of the venous and arterial pressures at S_v^o and S_a^o, respectively.

Hemodynamic Parameters

The use of CFD simulations makes it possible to also evaluate the classical hemodynamic parameters based on the wall shear stress. The wall shear stress WSS is defined as the modulus of the two-component vector

$$\boldsymbol{\tau}_w = \mu \frac{\partial \mathbf{v}}{\partial \mathbf{n}}, \quad (4)$$

where $\boldsymbol{\tau}_w$ is the viscous stress acting tangentially to the vessel wall and $\mathbf{n}$ the unit vector normal to the vessel wall. The time-averaged wall shear stress is defined as

Journal : CVET MS Code : 13239 PIPS No. : 185 ☐ TYPESET ☑ DISK ☐ LE ☑ CP Dispatch : 8-5-2014 Pages : 11

TABLE 1. Values of the venous and arterial resistances (R_v and R_a) and compliances (C_v and C_a) for the different values of time-averaged inlet pressure $\overline{P}_a^i$.

$\overline{P}_a^i$	$P_{a_s}^i$	$P_{a_d}^i$	R_a	C_a	R_v	C_v
55	63	51	11.9	4.98	4.77	11.5
70	78	66	30	5	6.5	12
90	98	86	41	5.04	7.4	12.1

The corresponding inlet pressures at peak systole $P_{a_s}^i$ and diastole $P_{a_d}^i$ are provided for reference. The pressures values are in mmHg, the resistances in $10^8 kg\,m^{-4}\,s^{-1}$ and the compliances in 10^8 kg m^{-4} s^{-1} kg^{-1} m^4 s^2.

$$\overline{WSS} = \frac{1}{T}\int_0^T |WSS| dt, \tag{5}$$

where T is the period of the cardiac cycle.

In a healthy radial artery, $\overline{WSS}$ is in the range 1–2 Pa,[37] which we will refer to as the healthy physiological WSS range. In a vein, it was reported that neointimal hyperplasia rapidly develops when WSS values are below 0.5 Pa.[20]

Validation

The solid and fluid solvers were validated independently. For the fluid solver, different mesh sizes were tested in order to guarantee a maximum error of 1% on the velocity magnitude and wall shear stresses and acceptable computational time t_{comp}. We investigated meshes of maximum element length $\Delta l_{\max}$ equal to 1, 2, 4, 5, 7 and 10×10^{-3} mm. The results obtained with the smallest mesh size (10^{-3} mm) were used as reference. In general, the relative error ε_u on the quantity u was defined as $|u - u^{ref}|/u^{ref}$. The relative error was calculated for $u = v_{\max}$, the maximum amplitude of the velocity vector $\mathbf{v}$ at the stenosis, and for $u = \overline{WSS}$, the time-averaged wall shear stress.

Figure 3 shows that the numerical procedure converged as $\Delta l_{\max}$ to the power 4.8 and that the normalized computational time decreased about linearly with $\Delta l_{\max}$. Hereafter, the results of the simulations are shown for a mesh characterized by a maximum element length of 4×10^{-3} mm, since it respects the 1%-error limit (horizontal line in Fig. 3a) for both the velocity and wall shear stress and runs four times faster than the reference case (Fig. 3b). The total number of elements used to mesh the blood lumen is then 7.84×10^5. A magnification of the mesh at the distal arterial outlet (S_a^2) is shown in Fig. 1.

The fluid solver was then further validated through comparison with measurements obtained *in vitro* in a rigid mold of the patient-specific AVF geometry. More details on the comparison can be found in Decorato *et al.*[9]

The solid solver was validated by modeling the inflation of a cylinder from radius R to radius $R(1 + \alpha)$ by an internal pressure P. A displacement was imposed to the shell, which induced a stretch ratio $\lambda = 1 + \alpha$. For a thin shell, an analytical solution can be derived relating the radial and tangential stresses to λ through the strain energy function.[17,35] Comparing the numerical results to the theoretical predictions, a precision of 1% was obtained when the arterial wall was discretized with 20 760 shell elements. A much smaller number of elements was needed to discretize the balloon (2100 shell elements), owing to its simple cylindrical geometry and smaller length.

RESULTS

Comparison of Pre- and Post-angioplasty Geometries

The success rate of the treatment by balloon-angioplasty is mainly measured by the change in cross-section of the stenosis. Figure 2e shows the evolution of the cross-sectional area A within the plane perpendicular to the flow direction that passes through the stenosis throat. The degree of residual stenosis is obtained by comparing the value of A with the average cross-section of the parent vessel upstream of the treated stenosis. From the cross-sectional area, one can calculate the equivalent vessel diameter D_{eq}, which is the diameter of the disk with the same cross-section:

$$D_{\text{eq}} = \sqrt{\frac{4A}{\pi}}. \tag{6}$$

Before treatment, $D_{\text{eq}} = 3.76$ (60% stenosis degree). After treatment, it is reduced to $D_{\text{eq}} = 4.97$, 5.31, 5.54 and 5.94 mm, when the stenosis is reduced to 30, 20, 10 and 0% respectively.

Comparison of Pre- and Post-angioplasty Hemodynamic Conditions

Results are first shown for an inlet mean pressure of $\overline{P}_a^i = 70$ mmHg. The influence of the boundary conditions will be examined in the next section.

Blood Flow

The streamlines, shown in Figs. 4a, 4b at peak systole for the patient-specific native (60% stenosis) and fully treated (0% stenosis) geometries respectively, provide a qualitative picture of the flow field distribution within the AVF. The flow field away from the stenosis appears not to be significantly influenced by the angioplasty treatment. This is confirmed by the comparison of the time-averaged flow rate at the venous outlet in the two cases: it is reduced by only 4%

Journal : CVET MS Code : 13239 PIPS No. : 185 ☐ TYPESET ☑ DISK ☐ LE ☑ CP Dispatch : 8-5-2014 Pages : 11

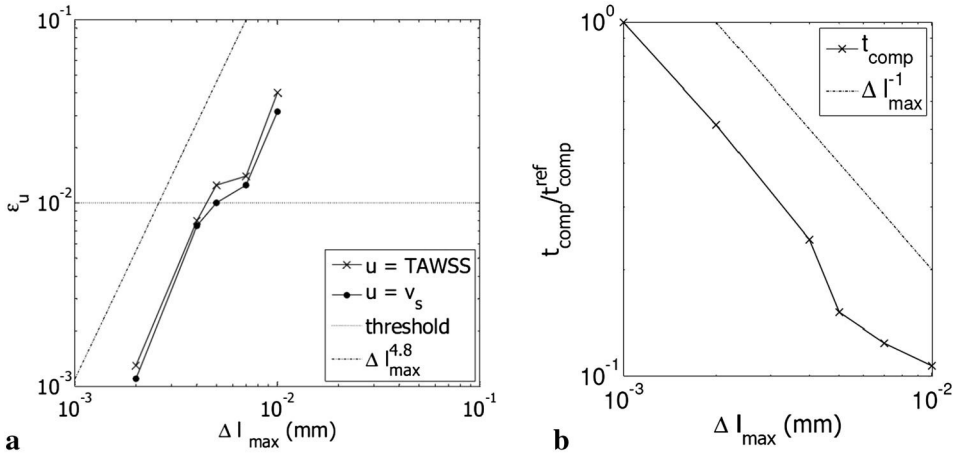

FIGURE 3. (a) Relative error on the maximum velocity ($\varepsilon_{v_{max}}$) and time-averaged wall shear stresses ($\varepsilon_{\overline{WSS}}$) as a function of the maximum mesh length Δl_{max}. The horizontal line indicates an error of 10^{-2}, chosen as the threshold. (b) Normalized computational time t_{comp}/t^{ref}_{comp} as a function of the maximum mesh length Δl_{max}. The reference case corresponds to the mesh with a maximum element length of 10^{-3} mm.

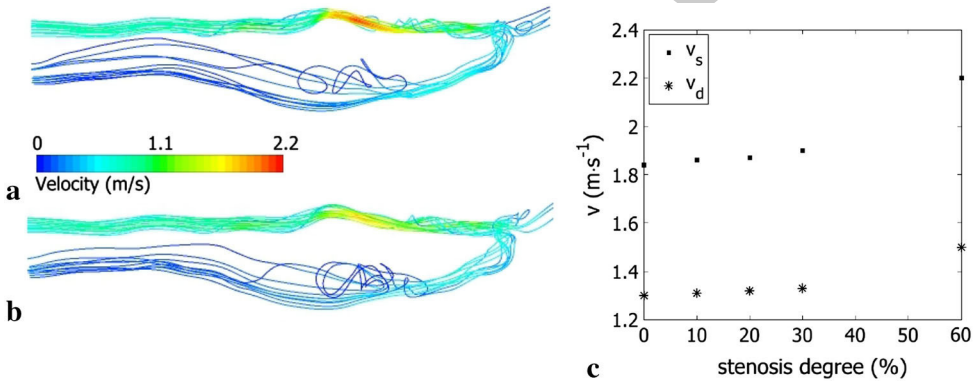

FIGURE 4. Streamlines at peak systole in the a) patient-specific and b) 0% residual stenosis geometries. c) Evolution of the peak systolic velocity v_s and late diastolic velocity v_d with the degree of residual stenosis.

when the arterial lumen cross-section is fully reopened. The main difference is observed locally at the stenosis, where the velocity magnitude is reduced following the removal of the stenosis. Figure 4c indicates the evolution of the peak systolic velocity v_s and late diastolic velocity v_d with the degree of residual stenosis. Both velocities follow a similar trend when the stenosis is treated and decrease by about 20%.

Wall Shear Stresses

Figures 5a, 5b show the spatial distribution of the time-averaged wall shear stress ($\overline{WSS}$) along the fistula wall for the patient-specific 60% stenosis) and fully treated (0% stenosis) geometries. Apart from the stenosis region, the WSS distribution is identical before and after treatment in the entire AVF geometry:

- The proximal and distal parts of the artery experience physiological values of $\overline{WSS}$ in the range 1-2 Pa.[37]
- The anastomosis experiences WSS one order of magnitude higher: the maximum instantaneous value is about 20 Pa.
- On the contrary, the vein experiences $\overline{WSS}$ values below 1 Pa or even 0.5 Pa in the dilated venous region.

Angioplasty, however, impacts the WSS in the stenosis region: Fig. 5c shows the $\overline{WSS}$ values at the stenosis location when the stenosis degree is corrected by angioplasty. After treatment, the $\overline{WSS}$ values are reduced from a maximum instantaneous value of 47 Pa (space-averaged value of 30 Pa) to nearly physiological values. Angioplasty treatment therefore has a pure local effect on the wall shear stresses. This is coherent with the fact that it has no influence on the overall flow distribution as shown in section 3.2.1.

Pressure Drop Across the Stenosis

The pressure drop across the stenosis is evaluated as the difference in average pressure between plane B_1,

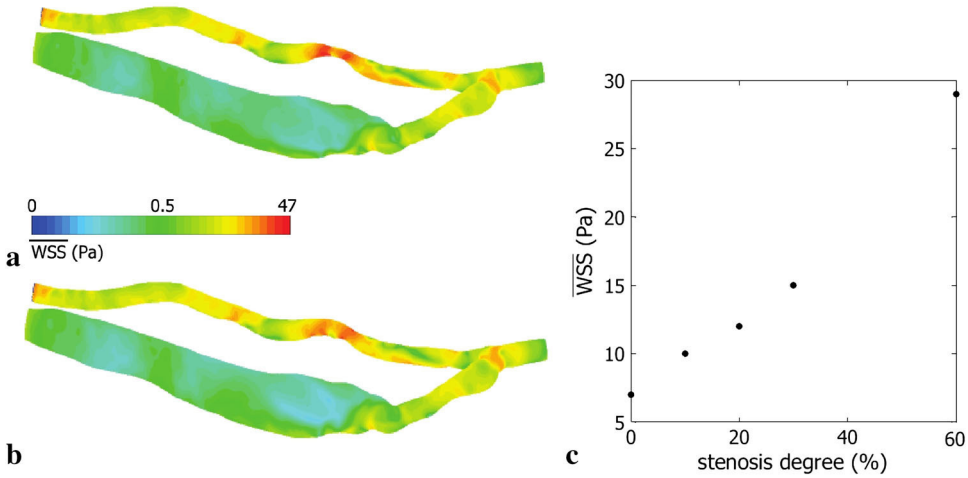

FIGURE 5. Spatial distribution of the time-averaged wall shear stress $\overline{WSS}$ for the (a) patient-specific and (b) 0% residual stenosis geometries. (c) Evolution of the time-averaged wall shear stress $\overline{WSS}$ at the stenosis throat with the stenosis degree.

located 1 mm upstream of the stenosis, and plane B_2, 1 mm downstream. The two planes are locally orthogonal to the main direction of the flow (Fig. 6a). Figure 6b shows the pressure drop $\overline{P}_{B_1}$ - $\overline{P}_{B_2}$ as a function of the degree of stenosis. The pressure drop across the stenosis increases with the degree of stenosis. It is interesting to notice that a degree of stenosis below 20% needs to be reached to have a pressure drop below 5 mmHg.

Effect of the Peripheral Vascular Boundary Conditions on the Hemodynamics Inside the AVF

The effect of varying the mean arterial pressure is investigated by changing the values of the resistance and compliance at the arterial and venous boundary conditions (Table 1). The values of resistance and compliance have been obtained maintaining the pulse pressure constant.

In Table 2 we compare the most important quantitative parameters: the value of the time-averaged venous blood flow, which is an indicator of the flow split between the distal artery and the vein, the peak systolic velocity at the stenosis and the pressure drop across the stenosis. We observe that none of the quantities are affected by the mean arterial pressure. The results therefore do not depend on the values set to the R and C constants in the Windkessel model.

DISCUSSION AND CONCLUSION

For the first time, the effects on the blood flow have been studied for a stenosis affecting the feeding artery of an arteriovenous fistula. The hemodynamics has been simulated numerically in a patient-specific AVF with an 60% arterial stenosis. The originality of the study is to model the removal of the stenosis by balloon-angioplasty through an implicit numerical simulation. The balloon is considered to be cylindrical when unloaded. The post-treatment geometry of the vessel is efficiently computed by mimicking the viscoplastic behavior of the arterial wall in the simulation. Since the stenosis removal is rarely complete in clinical practice, we have investigated different degrees of residual stenosis ranging from 30 to 0%. It is the range of stenosis correction that is considered as successful clinically.

To recreate physiologically realistic flow conditions, we have set patient-specific boundary conditions at the two outlets of the AVF using Windkessel models. The challenge was to design a technique to estimate the Windkessel model parameters from the flow rates, which were the only clinical data that could be measured non-invasively on the patient. Indeed no data existed in the literature on the global resistance and compliance of the arterial and the venous systems downstream of the AVF. If one compares the AVF values to the healthy case,[38] one finds that the venous compliance C_v is larger than in the healthy case by one order of magnitude at maximum, and that the venous resistance R_v is slightly smaller. Conversely, at the arterial side the compliance C_a is about 5 times smaller than in the healthy case and the resistance R_a is 8 times higher than the healthy case value. The R and C values calculated for the AVF translate the fact that the AVF redirects the flow preferentially into the vein.

To evaluate the influence of the arterial stenosis on the hemodynamics, we have compared the flow field within the patient-specific and treated geometries. We have shown that the arterial stenosis has no significant effect on the general hemodynamics within the AVF,

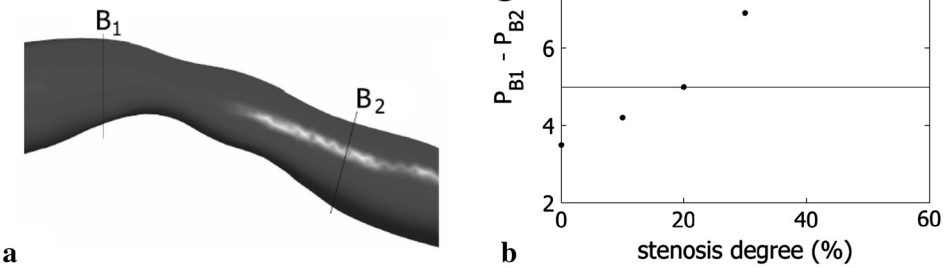

FIGURE 6. (a) Location of planes B_1 and B_2. (b) Stenosis pressure drop at the different degrees of residual stenosis. The horizontal line indicates the current clinical criterion, above which the lesion is treated by angioplasty.

TABLE 2. Comparison of the time-averaged venous blood flow $\overline{Q}_v$ at S_v^o, peak systolic velocity v_s and stenosis pressure drop in the patient-specific geometry, when the peripheral R and C values are modified.

$\overline{P}_a^i$ (mmHg)	**55**	**70**	**90**
$\overline{Q}_v$ (mL min^{-1})	750	752	754
v_s (m s^{-1})	2.20	2.20	2.20
$\overline{P}_{B_1} - \overline{P}_{B_2}$ (mmHg)	12.1	12	12

leaving unchanged the blood flow split between the distal artery and the vein. This is coherent with a recent study that showed that arterial stenoses only affect the arterial outflow when they are located within 5 mm from the anastomosis.[34] Our result explains why the fistula of the patient under study was still functioning despite the presence of an 60% stenosis: having no effect on the venous flow rate, the stenosis did not impact the efficiency of the hemodialysis treatment.

Various hemodynamic parameters have been computed to see whether they were influenced by the arterial stenosis:

Wall Shear Stresses

The presence of the stenosis leads to a local increase of the wall shear stresses at the stenosis neck. At this location, the time-averaged stress $\overline{WSS}$ is 5 times larger than in the fully corrected case (0%-stenosis)—see Fig. 5c. Singh *et al.*[33] have shown that a time-averaged stress of 15 Pa is the threshold, above which the endothelial cells are irremediably damaged and atherosclerotic plaques might form. From a *WSS* criterion, the present study indicates that the stenosis needs to be corrected with a degree of residual stenosis below 30% for the *WSS* to be below the threshold value of 15 Pa at the neck.

Pressure Drop Across the Stenosis

The pressure drop is the other hemodynamic parameter that was significantly influence by the presence of the arterial stenosis. This idea was already put forward by Young[41] for arterial stenoses in general. It is difficult to hypothesize what the clinical consequence of the increase in pressure drop will be. Will it lead to an increase in the upstream pressure and hence in the after-load cardiac pressure? If so, the necessity to remove the arterial stenosis is particularly high in AVF patients, who are already prone to heart failure and sudden cardiac death.[13,32] Does the increase in pressure drop instead lead to a decrease in the downstream pressure? It would then have a protecting heart effect. The urge to treat the arterial stenosis would be dictated by the fear of thrombosis and the necessity to preserve the AVF patency in the long-term.

All these results would need to be confirmed by other clinical studies. It would similarly be interesting to compare the predicted post-angioplasty geometry with the actual *in vivo* one. Although conducted on a single patient geometry, the present results can provide the basis for a reflection on the clinical criteria in the case of arterial stenosis. In clinics, a stenosis is currently treated when the pressure drop across the lesion is above 5 mmHg.[14] This criterion, originally set for venous stenoses, is used by default for arterial stenoses. We have found that a pressure drop of 5 mmHg corresponds to a 20% residual stenosis (Fig. 6b). The present study would therefore suggest that a 30% residual stenosis degree is too high for arterial stenoses and that the criterion for treatment needs to be reconsidered and adapted to the case of arterial stenosis. It could also be worth including the peak $\overline{WSS}$ in the reflection. But more cases would need to be studied to check whether the present results hold on.

Another point that needs to be improved is the detection of arterial stenoses. We have seen that arterial stenoses cause an increase in pressure drop in the concerned artery, but such a quantity is difficult to measure clinically. It could be of interest to investigate whether the formation of an arterial stenosis is associated with an increase in systemic pressure. If so the monitoring of the blood pressure evolution could become indicative of the presence of a stenosis, if changes are looked for over long time periods.

ACKNOWLEDGMENTS

This research is funded by the European Commission, through the MeDDiCA ITN (www.meddica.eu, Marie Curie Actions, grant agreement PITN-GA-2009-238113) and by the French Ministère de la Recherche (Pilcam2 grant). The authors gratefully acknowledge Polyclinique St Côme (Compiègne, FRANCE) for the medical images.

CONFLICT OF INTEREST

None.

STATEMENT OF HUMAN STUDIES

The clinical images were acquired in 2004 in conformity to the standards of use of medical images (patient consent, secured transfer of anonymized data).

STATEMENT OF ANIMAL STUDIES

N/A.

REFERENCES

[1]ANSYS Academic Research, Release 13.0, Help System. ANSYS Inc, 2010.

[2]Asif, A., F. N. Gadalean, D. Merrill, G. Cherla, C. D. Cipleu, D. L. Epstein, and D. Roth. Inflow stenosis in arteriovenous fistulas and grafts: a multicenter, prospective study. *Kidney Int*. 67:1986–1992, 2005.

[3]Asif, A. Endovascular procedures. *Contrib. Nephrol*. 161:30–38, 2008.

[4]Biuckians, A., B. C. Scott, G. H. Meier, J. M. Panneton, and M. H. Glickman. The natural history of autologous fistulas as first-time dialysis access in the k/doqi era. *J. Vasc. Surg*. 47:415–421, 2008.

[5]Bogert, L. W. J., and J. J. van Lieshout. Non-invasive pulsatile arterial pressure and stroke volume changes from the human finger. *Exp. Physiol*. 90:437–448, 2005.

[6]Chan, M. R., S. Bedi, R. J. Sanchez, H. N. Young, Y. T. Becker, P. S. Kellerman, and A. S. Yevzlin. Stent placement versus angioplasty improves patency of arteriovenous grafts and blood flow of arteriovenous fistulae. *Clin. J. Am. Soc. Nephrol*. 3:699–705, 2008.

[7]Coentrpo, L., and L. Turmel-Rodrigues. Monitoring dialysis arteriovenous fistulae: its in our hands. *J. Vasc. Access* 14(3):209–215, 2013.

[8]Corpataux, J. M., E. Haesler, P. Silacci, H. B. Ris, and D. Hayoz. Low-pressure environment and remodelling of the forearm vein in brescia-cimino haemodialysis access. *Nephrol. Dial. Transpl*. 17:1057–1062, 2002.

[9]Decorato, I., Z. Kharboutly, T. Vassallo, J. Penrose, C. Legallais, and A.-V. Salsac. Numerical simulation of the fluid–structure interactions in a compliant patient-specific arteriovenous fistula. *Int. J. Numer. Methods Biomed. Eng*. 30:143–159, 2014.

[10]Dixon, B. S. Why don't fistulas mature? *Kidney Int*. 70:1413–1422, 2006.

[11]Duijm, L. E. M., Y. S. Liem, R. van der Rijt, F. J. Nobrega, H. C. M. van der Bosch, P. Douwes-Draaijer, P. W. M. Cuypers, and A. V. Tielbeek. Inflow stenoses in dysfunctional hemodialysis access fistulas and grafts. *Am. J. Kidney Dis*. 48:98–105, 2006.

[12]Ene-Iordache, B., L. Mosconi, G. Remuzzi, and A. Remuzzi. Computational fluid dynamics of a vascular access case for hemodialysis. *J. Biomech. Eng*. 123:284–292, 2001.

[13]Fellstrm, B. C., A. G. Jardine, R. E. Schmieder, H. Holdaas, K. Bannister, J. Beutler, D.-W. Chae, A. Chevaile, S. M. Cobbe, C. Grnhagen-Riska, J. J. De Lima, R. Lins, G. Mayer, A. W. McMahon, H.-H. Parving, G. Remuzzi, O. Samuelsson, S. Sonkodi, G. Sleymanlar, D. Tsakiris, V. Tesar, V. Todorov, A. Wiecek, R. P. Wthrich, M. Gottlow, E. Johnsson, and F. Zannad. Rosuvastatin and cardiovascular events in patients undergoing hemodialysis. *N. Engl. J. Med*., 360:1395–1407, 2009.

[14]Forauer, A. R., E. K. Hoffer, and K. Homa. Dialysis access venous stenoses: treatment with balloon angioplasty1-versus 3-minute inflation times. *Radiology*, 249(1):375–381, 2008.

[15]Gasser, T. C., and G. A. Holzapfel. Finite element modeling of balloon angioplasty by considering overstretch of remnant non-diseased tissues in lesions. *Comput. Mech*. 40:47–60, 2007.

[16]Gervaso, F., C. Capelli, L. Petrini, S. Lattanzio, L. DiVirgilio, and F. Migliavacca. On the effects of different strategies in modelling balloon-expandable stenting by means of finite element method. *J. Biomech*. 41(6):1206–1212, 2008.

[17]Green, A. E., and J. E. Adkins. Large Elastic Deformations. Oxford University Press, 1970.

[18]Gutierrez, M. A., P. E. Pilon, S. G. Lage, L. Kopel, R. T. Carvalho, and S. S. Furuie. Automatic measurement of carotid diameter and wall thickness in ultrasound images. *Comput. Cardiol*. 29:359–362, 2002.

[19]Horl, W. H., K. M. Koch, C. Ronco, and J. F. Winchester. Replacement of renal function by dialysis. Kluwer Academic Publishers, 2004.

[20]Jackson, M., N. B. Wood, S. Zhao, A. Augst, J. H. Wolfe, W. M. W. Gedroyc, A. D. Hughes, S. A. M. c. G. Thom, and X. Y. Xu. Low wall shear stress predicts subsequent development of wall hypertrophy in lower limb bypass grafts. *Arter. Res*. 3:32–38, 2009.

[21]Kharboutly, Z. M. Fenech, J. M. Treutenaere, I. Claude, and C. Legallais. Investigations into the relationship between hemodynamics and vascular alterations in an established arteriovenous fistula. *Med. Eng. Phys*. 29(9):999–1007, 2007.

[22]Konner, K. History of vascular access for haemodialysis. *Nephrol. Dial. Transpl.* 20:2629–2635, 2005.
[23]Lee, T., and P. Roy-Chaudhury. Advances and new frontiers in the pathophysiology of venous neointimal hyperplasia and dialysis access stenosis. *Adv. Chronic Kidney Dis.* 16(5):329–338, 2009.
[24]Maher, E., A. Creane, S. Sultan, N. Hynes, C. Lally, and D. J. Kelly. Inelasticity of human carotid atherosclerotic plaque. *Ann. Biomed. Eng.* 39:2445–2455, 2011.
[25]Merril, E. W., and G. A. Pelletier. Viscosity of human blood: transition from Newtonian to non-Newtonian. *J. Appl. Physiol.* 23:178–182, 1967.
[26]Molino, P., C. Cerutti, C. Julien, G. Cusinaud, M. P. Gustin, and C. Paultre. Beat-to-beat estimation of wind-kessel model parameters in conscious rats. *Am. J. Physiol. Heart Circ. Phisiol.* 274:H171–H177, 1998.
[27]Niemann, A. K., S. Thrysoe, J. V. Nygaard, J. M. Hasenkam, and S. E. Petersen. Computational fluid dynamics simulation of a-v fistulas: From MRI and ultrasound scans to numeric evaluation of hemodynamics. *J. Vasc. Access* 24:ahead of print, 2011.
[28]Ozyer, U., A. Harman, E. Yildirim, C. Aytekin, F. Karakayali, and F. Boyvat. Long-term results of angioplasty and stent placement for treatment of central venous obstruction in 126 hemodialysis patients: a 10-years single-center experience. *Am. J. Roentgenol.* 193:1672–1679, 2009.
[29]Prendergast, P. J., C. Lally, S. Daly, A. J. Reid, T. C. Lee, D. Quinn, and F. Dolan. Analysis of prolapse in cardiovascular stents: a constitutive equation for vascular tissue and finite-element modelling. *J. Biomech. Eng.* 125:692–699, 2003.
[30]Rhie, C. M., and W. L. Chow. Numerical study of the turbulent flow past an airfoil with trailing edge separation. *AIAA J.* 21:1525–1532, 1983.
[31]Salman, L., M. Ladino, M. Alex, R. Dhamija, D. Merrill, O. Lenz, G. Contreras, and A. Asif. Accuracy of ultrasound in the detection of inflow stenosis of arteriovenous fistulae: results of a prospective study. *Semin. Dial.* 23:117–121, 2010.
[32]Sarnak, M. J. Cardiovascular complications in chronic kidney disease. *Am. J. Kidney Dis.* 41:11–17, 2003.
[33]Singh, P. K., A. Marzo, C. Staicu, M. G. William, I. Wilkinson, P. V. Lawford, D. A. Rufenacht, P. Bijlenga, A. F. Frangi, R. Hose, U. J. Patel, and S. C. Coley. The effects of aortic coarctation on cerebral hemodynamics and its importance in the etiopathogenesis of intracranial aneurysms. *J. Vasc. Int. Neurol.* 3:17–30, 2010.
[34]Swinnen, J. Duplex ultrasound scanning of the autogenous arterio venous hemodialysis fistula: a vascular surgeons perspective. *AJUM* 14:17–23, 2011.
[35]Timoshenko, S. P., and J. N. Goodier. Timoshenko and Gore: Theory of Elastic Stability: Theory of Elasticity. McGraw-Hill, 1970.
[36]Tordoir, J. H. M., H. G. Debruin, H. Hoeneveld, B. C. Eikelboom, and P. Kitslaar. Duplex ultrasound scanning in the assessment of arteriovenous fistulas created for hemodiafysis access—comparison with digital subtraction angiography. *J. Vasc. Surg.* 10:122–128, 1989.
[37]van Tricht, I., D. DeWachter, J. Tordoir, and P. Verdonk. Hemodynamics and complications encountered with arteriovenous fistulas and grafts as vascular access for hemodialysis: a review. *Ann. Biomed. Eng.* 33:1142–1157, 2005.
[38]Westerhof, N., F. Bosman, C. J. De Vries, and A. Noordergraaf. Analog studies of the human systemic arterial tree. *J. Biomech.* 2:121–143, 1969.
[39]Yeoh, O. H. Some forms of the strain energy function for rubber. *Rubber Chem. Technol.* 66:754–771, 1993.
[40]Yerdel, M. A., M. Kesence, K. M. Yazicuoglu ans, Z. Doseyen, A. G. Turkcapar, and E. Anadol. Effect of hemodynamic variables on surgically created arteriovenous fistula flow. *Nephrol. Dial. Transpl.* 12:1684–1688, 1997.
[41]Young, D. F. Fluid mechanics of arterial stenoses. *J. Biomech. Eng.* 101:157175, 1979.